A Hybrid Electromagnetics-Circuit Simulation Method Exploiting Discontinuous Galerkin Finite Element Time Domain Method

Ping Li, *Student Member, IEEE*, and Li Jun Jiang, *Member, IEEE*

***Abstract*—A hybrid electromagnetics (EM)-circuit simulation method employing the discontinuous Galerkin finite element time domain (DGFETD) method is developed to model single lumped port networks comprised of both linear and non-linear elements. The whole computational domain is split into two subsystems: one is the EM subsystem that is analyzed by DGFETD, while another is the circuit subsystem that is modeled by the Modified Nodal Analysis method to generate a circuit subsystem. The coupling between the EM and circuit subsystems is achieved through a lumped port. Due to the local properties of DGFETD operations, only small coupling matrix equation systems are involved. To handle non-linear devices, the standard Newton–Raphson method is applied to the established non-linear matrix equations. Numerical examples are presented to validate the proposed algorithm.**

***Index Terms*—DGFETD, hybrid EM-circuit simulator, MNA, non-linear, single port lumped circuit network, transient analysis.**

I. Introduction

RECENTLY, many transient simulators are available to analyze interactions between the full-wave and circuit regions. Among them, finite-difference time-domain (FDTD) method is popular for its simple implement. It considers lumped elements by a direct stamping technique [1], using an equivalent source concept [2], or an algorithm based on the admittance matrix in the Laplace domain [3].

TDFEM is another popular algorithm. In [4], TDFEM combined with MNA is employed to study the transient behavior of non-linear devices. A global system is constructed by coupling the full-wave parts with circuit subsystems. Special extraction technique is employed to construct a relatively small time-dependent matrix [4]. In [5], orthogonal vector basis functions are used to solve fully decoupled 1-D matrix directly with the reduction-recovery method.

Discontinuous Galerkin finite element time domain (DGFETD) method [6], [7] is recently extended to solve Maxwell equations. Due to the discontinuous property, all spatial operations of DGFETD are localized and solutions are allowed to be discontinuous across boundaries between neighboring elements. In [8], DGFETD is applied to study the transient behavior of interconnect structures with linear lumped elements by direct stamping technique. In [9], the lumped network is solved by a direct call of SPICE. Extra time is needed for the interface communication.

The aim of this letter is to develop a hybrid EM-circuit simulator to model arbitrary complex single port networks including both linear/non-linear elements. The EM part and circuit subsystem couple with each other through an lumped port. The EM part is analyzed by solving the Maxwell's equations via DGFETD, while the circuit part is modeled by MNA. At the lumped port, the coupling from the EM subsystem to the circuit subsystem is achieved by introducing a voltage source calculated by DGFETD, while the coupling from the circuit subsystem to the EM subsystem is realized by introducing a current source calculated by the circuit solver. The dimensions of the locally coupled matrix is equal to the number of degree of freedom in that mesh cell plus the number of unknowns in the circuit network. This local property is very important for circuit networks including nonlinear elements. To verify our algorithm, numerical results are presented.

II. Formulation

A. Formulation of DGFETD

Suppose that we are concerning the electromagnetic field in the computational domain Ω bounded by $\partial\Omega$. The global domain Ω is splitted into a set of non-overlapping subdomains Ω_i bounded by a surface $\partial\Omega_i$, where $\Omega = \bigcup \Omega_i$. Applying the discontinuous Galerkin testing procedure to the two first-order Maxwell's equations leads to the following two equations:

$$\int_{\Omega_i} \mathbf{\Phi}_k^{(i)} \cdot (\epsilon \frac{\partial \mathbf{E}}{\partial t} - \nabla \times \mathbf{H}) dV = \int_{\partial\Omega_i} \mathbf{\Phi}_k^{(i)} \cdot [\hat{\mathbf{n}} \times (\mathbf{H}^* - \mathbf{H}) - \mathbf{J}^{\mathrm{im}}] dS \quad (1)$$

$$\int_{\Omega_i} \mathbf{\Psi}_l^{(i)} \cdot (\mu \frac{\partial \mathbf{H}}{\partial t} + \nabla \times \mathbf{E}) dV = -\int_{\partial\Omega_i} \mathbf{\Psi}_l^{(i)} \cdot \hat{\mathbf{n}} \times (\mathbf{E}^* - \mathbf{E}) dS \quad (2)$$

where $\mathbf{\Phi}_k^{(i)}$ denotes the k-th vector basis function for $\mathbf{E}$ in the i-th subdomain and $\mathbf{\Psi}_l^{(i)}$ denotes the l-th vector basis function for $\mathbf{H}$ in the i-th subdomain. $\mathbf{J}^{\mathrm{im}}$ represents the imposed electrical current density in the EM subsystem. Here, it is assumed to be zero. $\hat{\mathbf{n}}$ is the unit normal vector pointing from the local element to the neighbor element. $\hat{\mathbf{n}} \times \mathbf{H}^*$ and $\hat{\mathbf{n}} \times \mathbf{E}^*$ called numerical flux are for communications between adjacent elements. In elements containing lumped ports, the central flux [8]

$$\hat{\mathbf{n}} \times \mathbf{H}^* = \hat{\mathbf{n}} \times \frac{\mathbf{H}^i + \mathbf{H}^j}{2} - \frac{\mathbf{J}^{\mathrm{CKT}}}{2} \quad (3)$$

Manuscript received August 21, 2012; revised December 18, 2012; accepted February 04, 2013. Date of publication February 21, 2013; date of current version March 07, 2013. This work is supported in part by the RGC of Hong Kong (GRF 711511 and 713011) and the UGC of Hong Kong (AoE/P-04/08).

The authors are with the Department of Electrical and Electronic Engineering, the University of Hong Kong, Hong Kong, China (e-mail: liping@eee.hku.hk, jianglj@hku.hk).

Color versions of one or more of the figures in this letter are available online at http://ieeexplore.ieee.org.

Digital Object Identifier 10.1109/LMWC.2013.2246149

$$\hat{\mathbf{n}} \times \mathbf{E}^* = \hat{\mathbf{n}} \times \frac{\mathbf{E}^i + \mathbf{E}^j}{2} \tag{4}$$

is employed, which is derived from the boundary condition over lumped ports. Namely, $\hat{\mathbf{n}} \times (\mathbf{H}^j - \mathbf{H}^i) = \mathbf{J}^{\mathrm{CKT}}$ and $\hat{\mathbf{n}} \times (\mathbf{E}^j - \mathbf{E}^i) = 0$. The superscripts j represent the neighboring element. $\mathbf{J}^{\mathrm{CKT}}$ denotes the current through the lumped port surface. At elements' boundary faces without lumped ports, the upwind flux [6], [7] is employed.

Next, the fields $\mathbf{E}$ and $\mathbf{H}$ in the domain Ω_i are expanded by local basis functions: $\mathbf{E} = \sum_{k=1}^{n_e^{(i)}} e_k^{(i)} \mathbf{\Phi}_k^{(i)}$, $\mathbf{H} = \sum_{l=1}^{n_h^{(i)}} h_l^{(i)} \mathbf{\Psi}_l^{(i)}$, where $n_e^{(i)}$ and $n_h^{(i)}$ are the number of degrees of freedom for $\mathbf{E}$ and $\mathbf{H}$ in the i-th domain, respectively. By substituting these two expressions together with (3) and (4) into (1) and (2), the EM matrix system in the elements where lumped ports reside can be constructed as

$$\mathbf{M}_e^{(i)} \frac{\partial \mathbf{e}^{(i)}}{\partial t} = \mathbf{S}_e^{(i)} \mathbf{h}^{(i)} - \frac{\mathbf{j}^{(i)}}{2} - \mathbf{F}_{eh}^{(ii)} \mathbf{h}^{(i)} + \mathbf{F}_{eh}^{(ij)} \mathbf{h}^{(j)} \tag{5}$$

$$\mathbf{M}_h^{(i)} \frac{\partial \mathbf{h}^{(i)}}{\partial t} = -\mathbf{S}_h^{(i)} \mathbf{e}^{(i)} + \mathbf{F}_{he}^{(ii)} \mathbf{e}^{(i)} - \mathbf{F}_{he}^{(ij)} \mathbf{e}^{(j)} \tag{6}$$

where $\mathbf{M}_{e/h}^{(i)}, \mathbf{S}_{e/h}^{(i)}$ are mass and stiffness matrices, respectively. $\mathbf{j}^{(i)}$, $\mathbf{F}_{eh}^{(ii)}$, $\mathbf{F}_{eh}^{(ij)}$, $\mathbf{F}_{he}^{(ii)}$ and $\mathbf{F}_{he}^{(ij)}$ are from numerical flux.

The first order time derivatives will be approximated using the centering difference method that is compatible with MNA. The fully discrete local system equations can be obtained from the semi-discrete system in (5) and (6) with the approximation $\mathbf{j}_{n+(1/2)}^{(i)} = (\mathbf{j}_{n+1}^{(i)} + \mathbf{j}_n^{(i)})/2$ as

$$\mathbf{M}_e^{(i)} \mathbf{e}_{n+1}^{(i)} = \mathbf{M}_e^{(i)} \mathbf{e}_n^{(i)} + \Delta t \left[\frac{\left(\mathbf{S}_e^{(i)} - \mathbf{F}_{eh}^{(ii)} \right) \mathbf{h}_{n+(1/2)}^{(i)} \left(\mathbf{j}_{n+1}^{(i)} + \mathbf{j}_n^{(i)} \right)}{4 + \mathbf{F}_{eh}^{(ii)} \mathbf{h}_{n+(1/2)}^{(j)}} \right] \tag{7}$$

$$\mathbf{M}_h^{(i)} \mathbf{h}_{n+(3/2)}^{(i)} = \mathbf{M}_h^{(i)} \mathbf{h}_{n+(1/2)}^{(i)} + \Delta t \left[\left(-\mathbf{S}_h^{(i)} + \mathbf{F}_{he}^{(ii)} \right) \mathbf{e}_{n+1}^{(i)} - \mathbf{F}_{he}^{(ij)} \mathbf{e}_{n+1}^{(j)} \right]. \tag{8}$$

B. Construction of Circuit Subsystem Equations With MNA

To generate circuit equations, MNA is employed to model single port lumped networks. The resultant circuit matrix equation at time $t = (n+1)\Delta t$ is

$$\begin{bmatrix} [\mathbf{Y}] & -[\mathbf{B}] \\ -[\mathbf{B}]^{\mathrm{T}} & \mathbf{0} \end{bmatrix} \begin{bmatrix} \mathbf{V}_{n+1}^{\mathrm{CKT}} \\ \mathbf{I}_{n+1}^{\mathrm{CKT}} \end{bmatrix} + \mathbf{I}_{n+1}^{\mathrm{CKT,nl}} \left(\mathbf{V}_{n+1}^{\mathrm{CKT}} \right) = \begin{bmatrix} \mathbf{I}_n^{\mathrm{CP}} \\ \mathbf{V}_{n+1}^{\mathrm{Port}} + \mathbf{V}_{n+1}^{\mathrm{ind}} \end{bmatrix} \tag{9}$$

where $[\mathbf{Y}]$ is determined by interconnections between the circuit elements, and $[\mathbf{B}]$ is determined by the connection of the supplied voltage sources. $\mathbf{V}_{n+1}^{\mathrm{CKT}}$ denotes the unknown non-reference node voltages, $\mathbf{I}_{n+1}^{\mathrm{CKT}}$ denotes the unknown currents through voltage sources. $\mathbf{I}_{n+1}^{\mathrm{CKT,nl}}$ represents currents through branches containing non-linear elements. $\mathbf{I}_n^{\mathrm{CP}}$ is comprised of both supplied current sources and those derived from companion models of inductors and capacitors, $\mathbf{V}_{n+1}^{\mathrm{Port}}$ holds the values of supplied voltage sources coupled from the EM part, while $\mathbf{V}_{n+1}^{\mathrm{ind}}$ represents the independent voltage source in the circuit subsystem. The overall dimensions of the circuit subsystem in (9), denoted as N^{CKT}, are equal to the number of non-reference voltage nodes plus the number of voltage sources.

C. Coupling Between the EM and Circuit Subsystems

The coupling between the EM and circuit subsystems is achieved by introducing impressed current and voltage sources at the rectangular lumped ports with width w and length l. Since the lumped port is small compared to the wavelength, quasi-static approximation is assumed at the lumped port. It means that the electric and magnetic fields are constant over the lumped port. At the time $t = (n+1)\Delta t$, the supplied voltage at the q-th lumped port associated to i-th element is determined by DGFETD and expressed as

$$\mathbf{V}_{n+1,q}^{\mathrm{Port}} = \sum_{p=1}^{n_e} e_{n+1,p}^{(i)} \int \mathbf{\Phi}_p^{(i)} \cdot \hat{l}_q dl = [C]_q^{(i)} \{e\}_{n+1}^{(i)} \tag{10}$$

where $\hat{l}_q$ is the unit vector along the direction of potential descending at the q-th port.

By combining (7), (9) and (10), the coupled local system equation can be established as

$$\mathbf{F}(\mathbf{x}_{n+1}) = \mathbf{b}_n \tag{11}$$

where

$$\mathbf{x}_{n+1} = [\mathbf{e}_{n+1}^{(i)} \quad \mathbf{V}_{n+1,q}^{\mathrm{CKT}} \quad \mathbf{I}_{n+1,q}^{\mathrm{CKT}}]^{\mathrm{T}} \tag{12}$$

$$\mathbf{F}(\mathbf{x}_{n+1}) = \begin{bmatrix} [\mathbf{M}_e^{(i)}] & \mathbf{0} & \frac{\Delta t \mathbf{G}_q^{(i)}}{4} \\ \mathbf{0} & [\mathbf{Y}]_q & -[\mathbf{B}]_q \\ [\mathbf{C}]_q^{(i)} & -[\mathbf{B}]_q^{\mathrm{T}} & \mathbf{0} \end{bmatrix} \begin{bmatrix} \mathbf{e}_{n+1}^{(i)} \\ \mathbf{V}_{n+1,q}^{\mathrm{CKT}} \\ \mathbf{I}_{n+1,q}^{\mathrm{CKT}} \end{bmatrix} + \begin{bmatrix} \mathbf{0} \\ \mathbf{I}_{n+1,q}^{\mathrm{CKT,nl}} \\ -\mathbf{V}_{n+1}^{\mathrm{ind}} \end{bmatrix} \tag{13}$$

$$\mathbf{b}_n = \begin{bmatrix} \mathbf{b}_{\mathrm{EM}} & \mathbf{I}_{n,q}^{\mathrm{CP}} & \mathbf{0} \end{bmatrix}^{\mathrm{T}} \tag{14}$$

with

$$\mathrm{G}_{q,k}^{(i)} = \frac{1}{w} \int_{\partial \Omega_{i,port}} \mathbf{\Phi}_k^{(i)} \cdot \hat{l}_q dS \tag{15}$$

$$\mathbf{b}_{\mathrm{EM}} = \mathbf{M}_e^{(i)} \mathbf{e}_n^{(i)} + \Delta t \left[\left(\mathbf{S}_e^{(i)} - \mathbf{F}_{eh}^{(ii)} \right) \mathbf{h}_{n+(1/2)}^{(i)} - \mathbf{I}_{n,q}^{\mathrm{CKT}} \frac{\mathrm{G}_q^{(i)}}{4} + \mathbf{F}_{eh}^{(ii)} \mathbf{h}_{n+(1/2)}^{(j)} \right]. \tag{16}$$

The overall dimensions of the coupled system in (11) are equal to $n_e^{(i)} + N^{\mathrm{CKT}}$. In our case, the EM domain is meshed into tetrahedrons. Each cell is assigned six vector edge basis functions ($n_e^{(i)} = 6$). Note that the minus sign in front of $[\mathbf{B}]$ is introduced since the current direction in our method is opposite to that defined in the standard MNA formulation. To tackle the instability issue caused by non-linear elements and get accurate solutions, the standard Netwon–Raphson method is used with trivial computational cost due to the small coupled matrix system.

The resultant marching scheme is explicit and conditionally stable. For the stability condition, the time-stepping size for the i-th element is chosen in terms of the following condition [8], [10]: $c_i \Delta t_i \left[(4\sqrt{5}/3) + (8/3)\max(\sqrt{(\mu_i/\mu_j)}, \sqrt{(\epsilon_i/\epsilon_j)}) \right] < P(4V_i/P_i)$, where $j \in N(i)$ represents the neighboring elements of the i-th element, $c_i = (1/\sqrt{\epsilon_i \mu_i})$ is the local light speed, P_i is the total area of four facets, and V_i is volume of element i. For the global stability, $\Delta t = \min(\Delta t_1, \Delta t_2, \ldots, \Delta t_N)$ is chosen. N is the total number of elements.

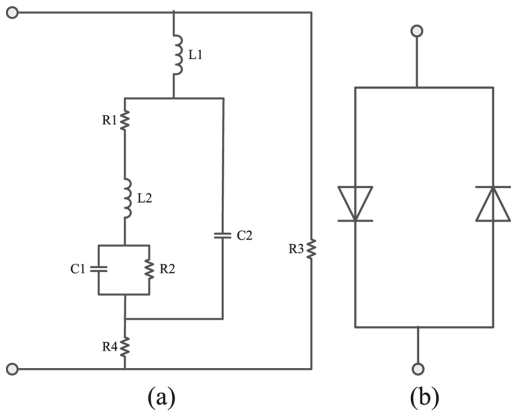

Fig. 1. (a) Lumped network including only linear elements, where $R_1 = 75\ \Omega$, $R_2 = 100\ \Omega$, $R_3 = 376.7\ \Omega$, $R_4 = 100\ \Omega$, $L_1 = 10$ nH, $L_2 = 1$ nH, $C_1 = 1$ pF, $C_2 = 0.01$ pF. (b) Two anti-parallel placed diodes.

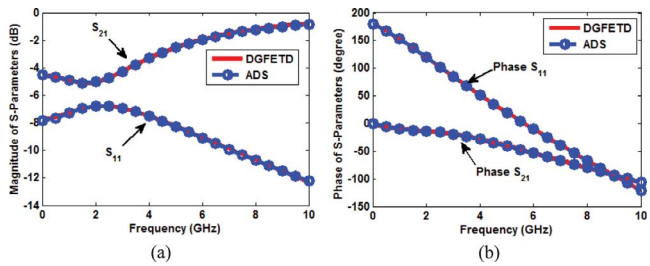

Fig. 2. Magnitude (a) and phase (b) of S_{11} and S_{21} calculated from the proposed hybrid EM-circuit simulator and ADS.

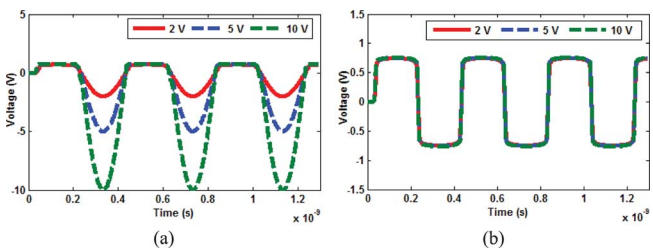

Fig. 3. Time domain voltage at the terminal of the diode corresponding to excitations with different amplitudes. (a) Output voltage of the single diode. (b) Output voltage of the diode pair.

III. Numerical Results

In the first example, a 1 cm parallel plate waveguide driven by a Thevenin voltage source and loaded by a lumped network comprised of only linear lumped elements as shown in Fig. 1(a) is studied. Two lumped ports are defined at the driving source and the load of the waveguide, respectively. The Thevenin voltage source is a first order differential Gaussian pulse. The dimensions of the coupled matrix of this lumped network are 13×13, including 6 field and 7 circuit unknowns. The time step size is 1.26×10^{-13} s. The amplitude and phase of S parameters are presented in Fig. 2. It is observed that very good agreement is achieved.

In the next example, the same parallel plate waveguide driven by a TEM wave is studied. The same mesh structure as the former example is employed, which means the same time step size. The two ends of this waveguide are truncated by the first order absorbing boundary condition. In this case, it is loaded with a silicon diode $(i_D(t) = I_0[e^{V_D(t)/V_0} - 1], I_0 = 10^{-14}\ \text{A}, V_0 = 0.026\ \text{V})$. Since it is a nonlinear device, the Newton–Raphson method is applied to solve the nonlinear matrix equations. The incident wave is a sinusoidal source oscillating at 2.5 GHz. The amplitude of this sinusoidal source is gradually increased. The time domain voltage of the diode is presented in Fig. 3(a) with no instability problem. It can be noted that the maximum voltage at the diode terminal is around 0.7 V, which complies with the theory. Finally, a diode pair shown in Fig. 1(b) is used as the waveguide load. This diode pair is capable of limiting the output voltage. Theoretically, the output voltage should be between -0.7 V and 0.7 V. To verify the validity of the proposed algorithm, the output voltage at this diode pair is shown in Fig. 3(b). The calculated result agrees with the theory perfectly.

IV. Conclusion

In this letter, a hybrid EM-circuit simulator based on DGFETD and MNA is developed to model single port lumped networks. Interactions between the EM and circuit systems are achieved through a lumped port residing over a rectangular surface. Due to the local property of DGFETD, the resultant coupled EM-circuit system is very small. Hence, it can be solved efficiently, even nonlinear elements are included. When nonlinear elements are involved, the Newton–Raphson method is applied to the matrix equation. The proposed algorithm is validated by numerical examples.

Acknowledgment

The authors wish to thank Dr. W. C. Chew for constructive suggestions and the reviewers for valuable comments.

References

[1] M. Piket-May, A. Taflove, and J. Baron, "FD-TD modeling of digital signal propagation in 3-D circuits with passive and active loads," *IEEE Trans. Microw. Theory Tech.*, vol. 42, no. 8, pp. 1514–1523, Aug. 1994.

[2] C. N. Kuo, R. B. Wu, B. Houshmand, and T. Itoh, "Modeling of microwave active devices using the FDTD analysis based on the voltage-source approach," *IEEE Microw. Guided Wave Lett.*, vol. 6, pp. 199–201, Apr. 1996.

[3] C. C. Wang and C. W. Kuo, "An efficient scheme for processing arbitrary lumped multiport devices in the finite-difference time-domain method," *IEEE Trans. Microw. Theory Tech.*, vol. 55, no. 5, pp. 958–965, May 2007.

[4] R. Wang and J. M. Jin, "A symmetric electromagnetic-circuit simulator based on the extended time-domain finite element method," *IEEE Trans. Microw. Theory Tech.*, vol. 56, no. 12, pp. 2875–2884, Dec. 2008.

[5] Q. He and D. Jiao, "Fast electromagnetic-based co-simulation of linear network and nonlinear circuits for the analysis of high-speed integrated circuits," *IEEE Trans. Microw. Theory Tech.*, vol. 58, no. 12, pp. 3677–3687, Dec. 2010.

[6] X. Li and J. M. Jin, "A comparative study of three finite element-based explicit numerical schemes for solving Maxwell's equations," *IEEE Trans. Antennas Propag.*, vol. 60, no. 3, pp. 1450–1457, Mar. 2012.

[7] F. G. Hu and C. F. Wang, "Modeling of waveguide structures using DG-FETD method with higher order tetrahedral elements," *IEEE Trans. Microw. Theory Tech.*, vol. 60, no. 7, pp. 2046–2054, Jul. 2012.

[8] S. Dosopoulos and J. F. Lee, "Interconnect and lumped elements modeling in interior penalty discontinuous Galerkin time-domain methods," *J. Comput. Phys.*, vol. 229, pp. 8521–8536, Aug. 2010.

[9] B. Zhao, J. C. Yong, and S. D. Gedney, "SPICE lumped circuit subcell model for the discontinuous Galerkin finite element time-domain method," in *Proc. IEEE Int. Symp. Antennas Propag.*, Jul. 2011, pp. 2269–2271.

[10] L. Fezoui, S. Lanteri, S. Lohrengel, and S. Piperno, "Convergence and stability of a discontinuous Galerkin time-domain method for the 3D heterogeneous Maxwell equations on unstructured meshes," in *Proc. ESAIM: M2AN*, 2005, pp. 1149–1176.